Interaction and Multiscale Mechanics, Vol. 5, No. 4 (2012) 347-368
DOI: http://dx.doi.org/10.12989/imm.2013.5.4.347

Effect of road surface roughness on the response of a moving vehicle for identification of bridge frequencies

Y.B. Yang*, Y.C. Li and K.C. Chang

Department of Civil Engineering, National Taiwan University, Taipei, Taiwan

(Received October 15, 2012, Revised October 30, 2012, Accepted November 15, 2012)

Abstract. Measuring the bridge frequencies indirectly from an instrumented test vehicle is a potentially powerful technique for its mobility and economy, compared with the conventional direct technique that requires vibration sensors to be installed on the bridge. However, road surface roughness may pollute the vehicle spectrum and render the bridge frequencies unidentifiable. The objective of this paper is to study such an effect. First, a numerical simulation is conducted using the vehicle-bridge interaction element to demonstrate how the surface roughness affects the vehicle response. Then, an approximate theory in closed form is presented, for physically interpreting the role and range of influence of surface roughness on the identification of bridge frequencies. The latter is then expanded to include the action of an accompanying vehicle. Finally, measures are proposed for reducing the roughness effect, while enhancing the identifiability of bridge frequencies from the passing vehicle response.

Keywords: bridge; frequency; identification; surface roughness; vehicle; vehicle-bridge interaction.

1. Introduction

Conventionally, the identification of bridge frequencies requires the installation of vibration sensors directly deployed on the bridge. Such an approach is called the direct approach and is the one that is frequently adopted by researchers and engineers. In contrast, a second approach called the indirect approach was proposed by Yang *et al*. (2004) for identifying the bridge frequencies, by recording the acceleration response of an instrumented test vehicle during its passage over the bridge of concern, and then by extracting the bridge frequencies from the vehicle response spectrum. With this approach, no vibration sensors need to be mounted on the bridge.

Previous research on identification of bridge frequencies by the direct approach has been voluminous. The following is only a partial review. Abdel-Ghaffer and Scanlan (1985) identified the modal parameters of the Golden Gate Bridge using the ambient vibrations tests along with the peak-picking method. Wilson and Liu (1991) performed microvibration tests on the Quincy Bayview Bridge in Illinois, using the accelerators installed on the bridge deck to record the vertical, torsional and transverse vibrations. The bridge frequencies were also identified by the peak-picking method, which compared well with the finite element analysis results. Due to the advancement in

* Corresponding author, Professor, E-mail: ybyang@ntu.edu.tw

measurement devices and analysis methods, system identification of bridge modal properties has received increasing attention from researchers in the past two decades. Ren *et al*. (2004) used both the peak-picking method and stochastic subspace identification method to identify from the field measurement data the frequencies and modal shapes of the Tennessee River Bridge, a nine-span steel arch bridge, and compared their results with the finite element analyses. He *et al*. (2009) conducted a system identification study on the Alfred Zampa Memorial Bridge using the dynamic field test data. Recently, Brownjohn *et al*. (2010) conducted an ambient vibration re-testing and operational modal analysis of the Humber Bridge.

The idea of using an instrumented vehicle to measure the bridge frequencies was proposed by Yang *et al*. (2004) in 2004 after a long period of research on the vehicle-bridge interaction problems. This idea was experimentally verified to be feasible by Lin and Yang (2005), along with the potential applications of vehicle-bridge interaction properties identified (Yang and Lin 2005). Extended studies along these lines include those of Bu *et al*. (2006), McGetrick *et al*. (2009), Yang and Chang (2009a, 2009b), Chang *et al*. (2010), Xiang *et al*. (2010) and Nguyen and Tran (2010).

From the above brief review, it is realized that the direct approach is a rather mature technique. By installing vibration sensors on a bridge, various techniques can be utilized to identify the dynamic parameters of a bridge. However, using such an approach, the deployment of vibration sensors on the bridge is generally costly and laborious. For example, the field study of the Quincy Bayview Bridge had required a team of four persons to work for five days in the field (Wilson and Liu 1991). Obviously, the cost and labor required by the direct approach have made it not a feasible approach for monitoring a large number of bridges in a short time for the purpose of damage-detection, say, after a major earthquake. In comparison, the indirect approach has the potential of becoming an effective tool for periodically monitoring the frequencies of a large number of bridges for its mobility, promptness and economy, although there remain some technical problems to be resolved.

This paper is focused on the effect of road surface roughness that is critical to the extraction of bridge frequencies from the recorded acceleration response of the passing test vehicle. First, numerical simulations are conducted using the vehicle-bridge interaction elements to demonstrate the blurring effect of road surface roughness. Then, an approximate theory in closed form is presented for physically interpreting and assessing the role and range of influence of road surface roughness. Finally, some measures are proposed for reducing or eliminating the effect of road surface roughness in the vehicle response spectrum, so as to enhance the visibility of bridge frequencies in field applications.

2. Simulation of roughness profiles

The power spectral density (PSD) functions defined by ISO 8608 (1995) for the road surface profiles will be adopted herein. According to this specification, the road surface is divided into eight classes, with Class A indicating the best surface and Class H the poorest. The PSD function $G_d(n)$ for the surface profile is defined as

$$G_d(n) = G_d(n_0)\left(\frac{n}{n_0}\right)^{-w} \tag{1}$$

where n denotes the spatial frequency per meter, w is a constant equal to 2, $n_0 = 0.1$ cycle/m, and

the functional value $G_d(n_0)$ is determined by the roughness class, as given in ISO 8608 (1995). The amplitude d for each class of roughness selected is determined by

$$d = \sqrt{2G_d(n)\Delta n} \tag{2}$$

where Δn is the sampling interval of the spatial frequency. However, the amplitude of roughness so obtained is too large to be compatible with the road roughness from the field. For this reason, a square root is taken of the geometric mean of the functional value provided by ISO 8608 (1995) in this study. Besides, to simulate the perfect surface condition, i.e., roughness level A, a very small value of 0.001×10^{-6} is assigned for the functional value (geometric mean) of the class without taking the square root. Consequently, the functional values adopted for the three classes of roughness in this study are: Class A: $G_d^*(n_0) = 0.001 \times 10^{-6}\text{m}^3$; Class B: $G_d^*(n_0) = \sqrt{64} \times 10^{-6}\text{m}^3$ and Class C: $G_d^*(n_0) = \sqrt{256} \times 10^{-6}\text{m}^3$.

Then, the road surface roughness can be superimposed as follows

$$r(x) = \sum_i d_i \cos(n_{s,i}x + \theta_i) \tag{3}$$

where $n_{s,i}$ is the ith spatial frequency considered, and d_i and θ_i denote the amplitude, as given in Eq. (2), and the random phase angle, respectively, of the ith cosine function. In this study, the sampling interval Δn_s for the spatial frequency is taken as 0.04 cycle/m, and the range of spatial frequency n_s is taken as 1 - 100 cycle/m.

3. Simulation of bridges with rough surface

In this section, the procedure for simulating the vehicle-bridge interaction (VBI) system and for considering the road surface roughness by the finite element method is summarized. For illustration, only simply supported bridges are considered, and the vehicle is modeled as a single degree-of-freedom (DOF) mass supported by a spring-dashpot unit. In the numerical simulation, a bridge is divided into a number of finite elements, each of 6 DOFs for the present two-dimensional case.

For an element of length l directly under the action of the vehicle, it is modeled as a VBI element with the effects of vehicle action and surface roughness included (see Fig. 1). The equation of motion for the VBI element is (Chang *et al*. 2010)

$$\begin{bmatrix} m_v & 0 \\ 0 & [\mathbf{m_b}] \end{bmatrix} \begin{Bmatrix} \ddot{q}_v(t) \\ \{\ddot{\mathbf{q}}_\mathbf{b}(t)\} \end{Bmatrix} + \begin{bmatrix} c_v & -c_v\{\mathbf{N}(x_c)\}^T \\ -c_v\{\mathbf{N}(x_c)\} & [\mathbf{c_b}] + c_v\{\mathbf{N}(x_c)\}\{\mathbf{N}(x_c)\}^T \end{bmatrix} \begin{Bmatrix} \dot{q}_v(t) \\ \{\dot{\mathbf{q}}_\mathbf{b}(t)\} \end{Bmatrix}$$

$$+ \begin{bmatrix} k_v & -k_v\{\mathbf{N}(x_c)\}^T - c_v v[\{\mathbf{N}'(x)\}^T]\big|_{x=x_c} \\ -k_v\{\mathbf{N}(x_c)\} & [\mathbf{k_b}] + c_v v\{\mathbf{N}(x_c)\}[\{\mathbf{N}'(x)\}^T]\big|_{x=x_c} + k_v\{\mathbf{N}(x_c)\}\{\mathbf{N}(x_c)\}^T \end{bmatrix} \begin{Bmatrix} q_v(t) \\ \{\mathbf{q}_\mathbf{b}(t)\} \end{Bmatrix}$$

$$= \begin{Bmatrix} c_v v r'(x)\big|_{x=x_c} + k_v r(x_c) \\ -c_v[r'(x)]\big|_{x=x_c}\{\mathbf{N}(x_c)\} - k_v r(x_c)\{\mathbf{N}(x_c)\} - m_v g\{\mathbf{N}(x_c)\} \end{Bmatrix} \tag{4}$$

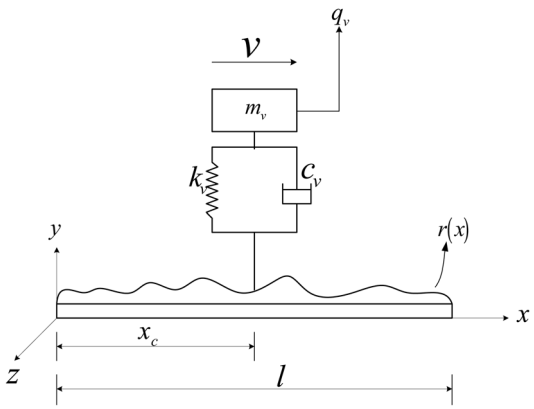

Fig. 1 Vehicle-bridge interaction element with surface roughness

where the parameters related to the vehicle are: q_v = vertical displacement, m_v = lumped mass, c_v, k_v = damping and stiffness coefficients of the suspension system, and v = speed; the parameters related to the bridge element are: $\{\mathbf{q_b}\}$ = vector of the nodal DOFs, $[\mathbf{m_b}]$, $[\mathbf{c_b}]$, $[\mathbf{k_b}]$ = mass, damping and stiffness matrices, and $\{\mathbf{N}\}$ = cubic Hermitian interpolation functions; g = acceleration of gravity; $r(x)$ = profile of road surface; x_c = contact position of the vehicle on the element; and a prime and overdot denote respectively differentiation of the quantity with respect to coordinate and time.

The term on the right-hand side of Eq. (4) represents the contact or interaction forces between the vehicle and bridge caused by the vehicle weight, $-m_v g\{N(x_c)\}$, and road surface roughness $r(x)$. In particular, the road surface roughness $r(x)$ affects only the contact forces, but not the system matrices appearing on the left-hand side of Eq. (4). Evidently, the presence of road surface roughness does not alter the frequency contents of the whole VBI system.

For the remaining parts of the bridge that are not directly acted upon by the vehicle, they are modeled by the conventional 6-DOF beam elements, of which the equation of motion is

$$[\mathbf{m_b}]\{\ddot{\mathbf{q}}_\mathbf{b}\} + [\mathbf{c_b}]\{\dot{\mathbf{q}}_\mathbf{b}\} + [\mathbf{k_b}]\{\mathbf{q_b}\} = \{\mathbf{0}\} \tag{5}$$

where each of the terms has already been defined following Eq. (4). By the finite element procedure of assembly, the equation of motion can be established for the whole VBI system as

$$[\mathbf{M}]\{\ddot{\mathbf{u}}\} + [\mathbf{C}]\{\dot{\mathbf{u}}\} + [\mathbf{K}]\{\mathbf{u}\} = \{\mathbf{P}\} \tag{6}$$

where $[\mathbf{M}]$, $[\mathbf{C}]$ and $[\mathbf{K}]$ denote respectively the mass, damping and stiffness matrices of the system, and $[\mathbf{P}]$ denotes the forces acting on the system. In this study, the preceding equation will be solved by the Newmark-β method with constant average acceleration (i.e., with $\beta = 1/4$ and $\gamma = 1/2$) for its unconditional stability.

4. Effect of surface roughness on vehicle response

Three classes of surface roughness, i.e., Classes A-C, will be considered for the bridge that is to be traveled by the test vehicle. The properties adopted for the vehicle lumped as a single-DOF

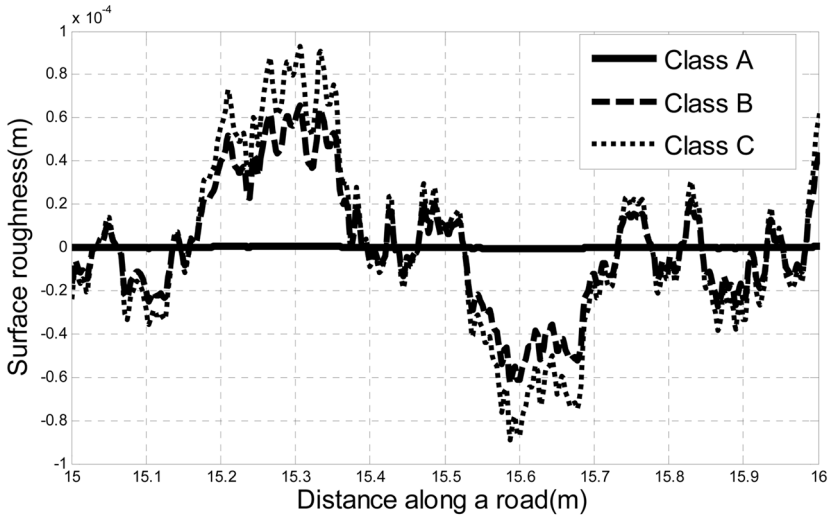

Fig. 2 A segment of road surface profile generated

sprung mass shown in Fig. 1 are: $m_v = 1000$ kg, $k_v = 170$ kN/m and $v = 2$ m/s. The bridge simply supported at both ends is divided into 20 elements with the following properties: elastic modulus $E = 27.5$ GPa, moment of inertia $I_b = 0.175$ m^4, mass per unit length $\overline{m} = 1000$ kg/m and cross-sectional area $A = 2$ m^2.

As was mentioned previously, the functional values $G_d(n_0)$ to be used for the PSD function $G_d(n)$ in Eq. (1) are modified from the geometric means provided by ISO 8608 (1995) as 0.001×10^{-6}, 8×10^{-6} and 16×10^{-6}, respectively, for roughness Classes A, B and C. A segment of the surface profile of roughness generated using Eq. (3), along with Eqs. (2) and (1), for each of three classes has been plotted in Fig. 2.

4.1 Case 1: Vehicle frequency less than any bridge frequencies

With the above assumed data, the vehicle frequency computed is less than any of the bridge frequencies.

Figs. 3(a)-(c) show the time-history acceleration response and frequency spectrum of the test vehicle during its passage over the bridge for the three classes of road surface considered. The observations are as follows: For road surface of the best quality, i.e., Class A, the first three bridge frequencies, i.e., 3.867, 15.27 and 34.3 Hz, can be clearly identified, along with the vehicle frequency of 2.067 Hz. For road surface of the second best quality, i.e., Class B, only the first bridge frequency can be identified, along with the vehicle frequency. And for the poorest road surface, i.e., Class C, the only frequency that can be identified is the vehicle frequency, while all the bridge frequencies have been completely hidden. From this analysis, it is clear that road surface roughness is an effect of crucial importance in identifying the bridge frequencies from the vehicle response spectrum. It is concluded that the rougher the road surface, the less number of bridge frequencies can be identified, or the higher the difficulty exists for identifying the bridge frequencies.

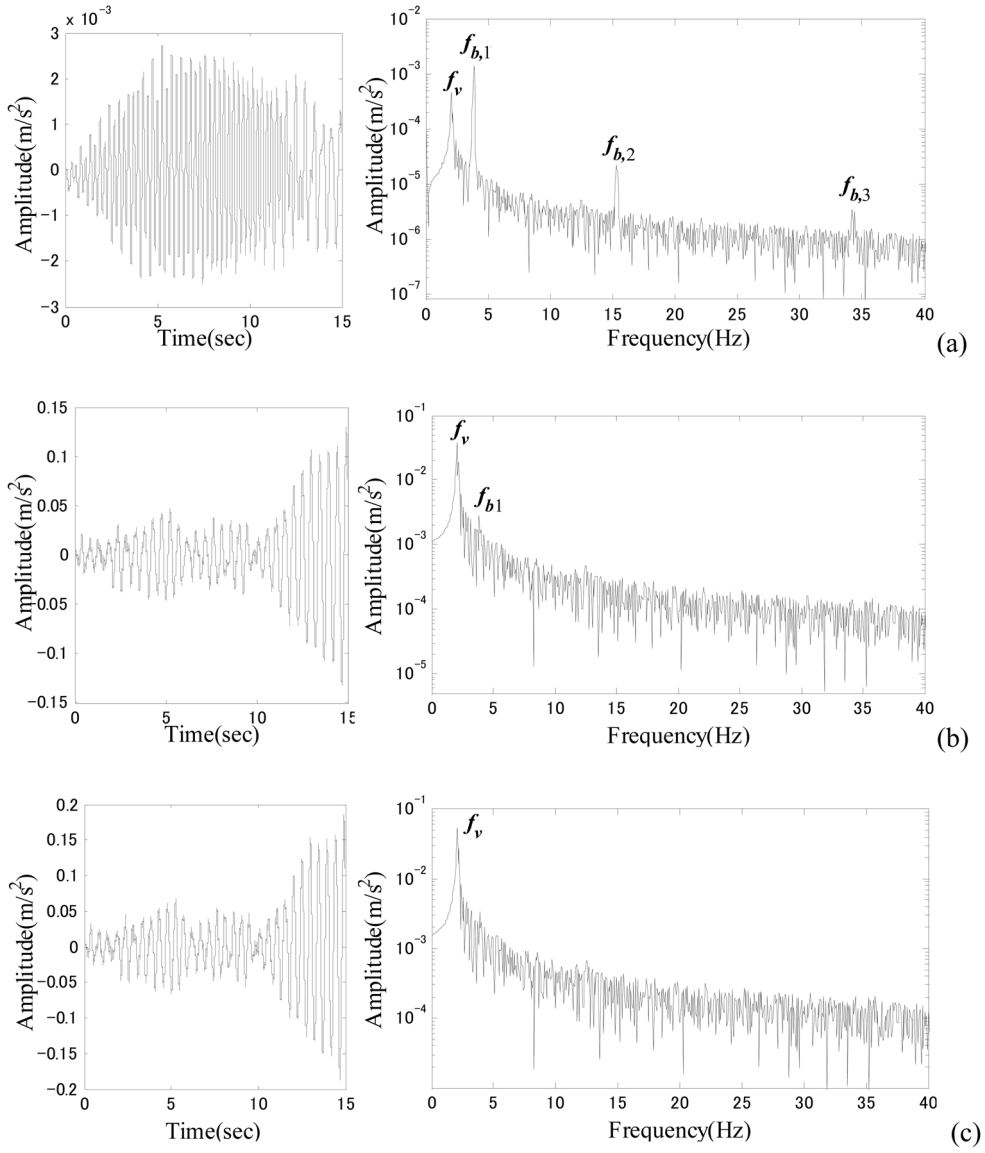

Fig. 3 Acceleration and frequency responses of test vehicle for Class: (a) A, (b) B and (c) C

4.2 Case 2: Vehicle frequency greater than the first bridge frequency

The above analysis has been conducted for the case when the vehicle frequency is smaller than any of the bridge frequencies. To evaluate the effect of the vehicle/bridge frequency ratio, one considers herein another case with the vehicle frequency significantly higher than the first frequency of the bridge. In other words, the vehicle frequency is raised from 2.067 to 10 Hz by increasing the vehicle stiffness from 170 to 3.947 MN/m, the other properties remaining unchanged. For this case, the time-history acceleration response and frequency spectrum solved of the test vehicle during its

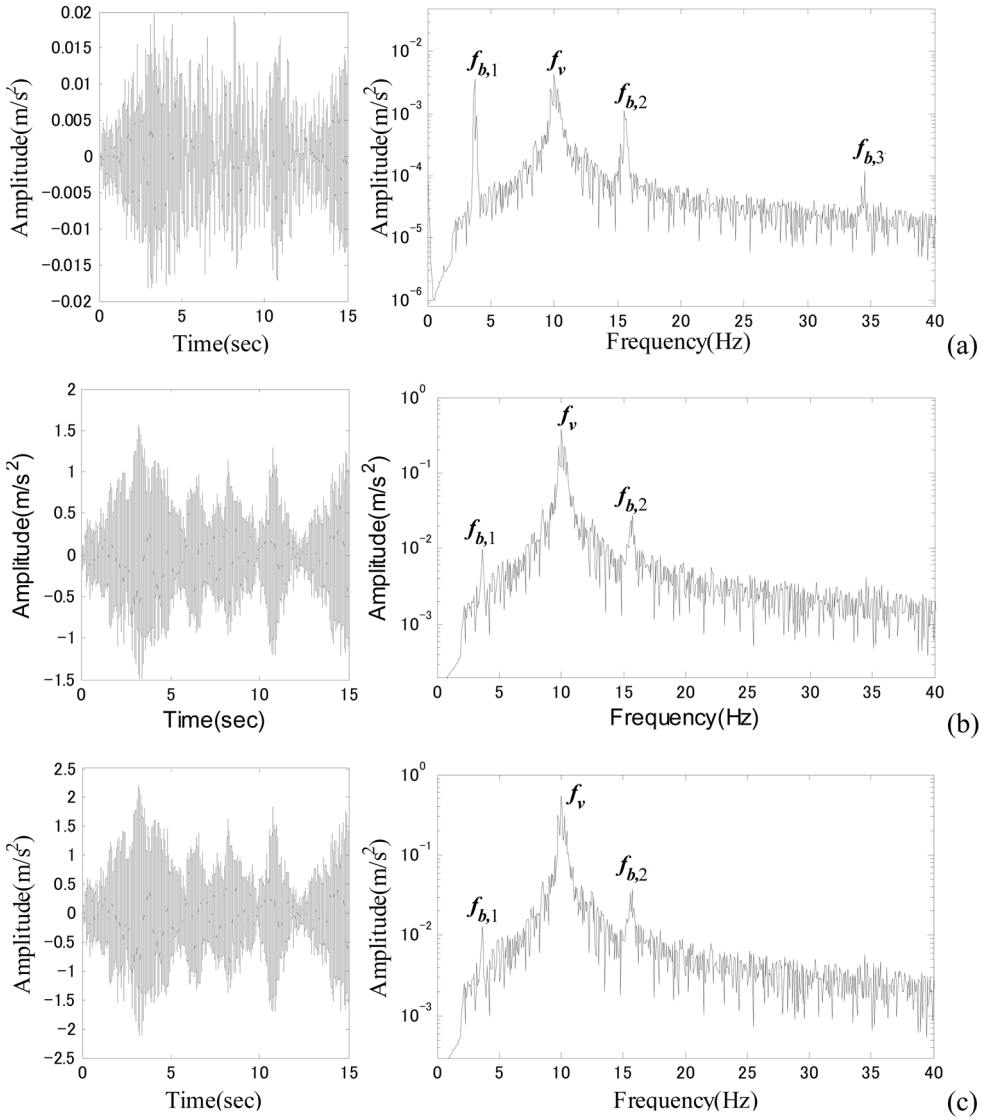

Fig. 4 Acceleration and frequency responses of test vehicle for Class: (a) A, (b) B and (c) C

passage over the bridge for the three classes of roughness considered have been plotted in Figs. 4(a)-(c).

An observation from Figs. 4(a)-(c) is that the amplitude of the vehicle frequency and roughness frequencies are amplified as the roughness level increases. Moreover, the third bridge frequency is hidden for Class B and C, while the amplitudes of the first and second bridge frequency appear to be generally visible. Further, by comparing Figs. 4 with 3, one observes that in Case 1 only the first bridge frequency remains visible for all three classes of roughness, while in Case 2, both the first and second bridge frequencies are visible for all classes of roughness considered. Thus, from the point of practice, it is advantageous to use a test vehicle with a frequency "greater than" the first

frequency of the bridge, in order to increase the visibility of bridge frequencies. In general, the above analyses also indicate that bridge frequencies of higher modes may be blurred or hidden by the presence of roughness, which therefore is crucial to the successful identification of bridge frequencies using the test vehicle.

5. Vehicle responses induced by separate excitational sources

For a test vehicle moving over a bridge that is initially at rest, the bridge will be set in motion by the moving test vehicle. Due to the interaction between the two subsystems, the test vehicle will be excited by the bridge as well during its passage over the bridge. If the bridge has a rough surface, then the test vehicle will also be excited by the surface roughness in a spatially random manner. To assess how the road surface roughness produces a blurring effect on the bridge frequencies in the vehicle response spectrum, we can separate the two excitational sources and study the dynamic response of the test vehicle under each of the following two extreme cases:

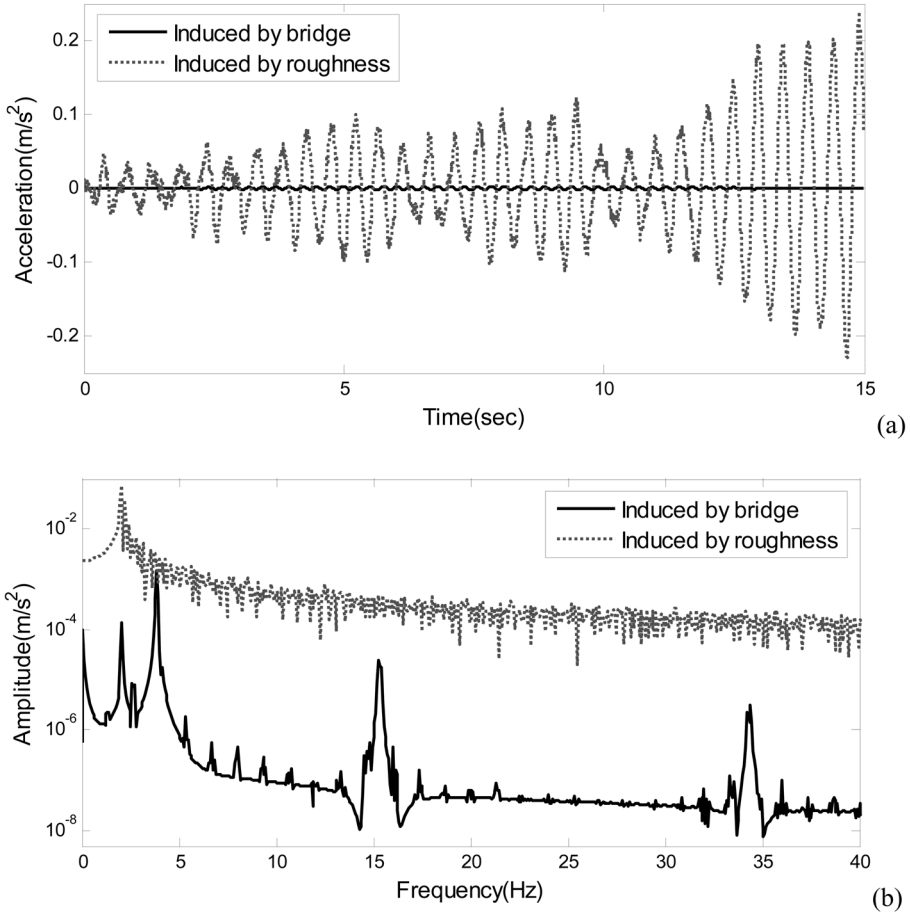

Fig. 5 Acceleration responses of the vehicle: (a) time history and (b) amplitude spectrum

(1) The test vehicle moving over a bridge with smooth road surface: In this case, the vehicle is excited exclusively by the vibration of the bridge.
(2) The vehicle moving over a bridge of an infinitely large flexural rigidity, but with rough surface: In this case, the vehicle is excited by the road surface roughness only.

Figs. 5(a) and (b) show the vehicle acceleration response and Fourier spectrum, respectively, for the above two cases. As can be seen, the vehicle is excited much more dramatically by the surface roughness than by the bridge in vibration. This explains why substantial difficulty exists in extracting bridge frequencies from the vehicle response spectrum, once the road surface roughness is taken into account. Clearly, two approaches can be adopted to resolve such a problem.

One approach is to increase the vibration amplitude or energy of the bridge by allowing the bridge to be exposed to existing traffic or accompanying vehicles. In fact, it was demonstrated that the existence of ongoing traffic or accompanying vehicles is beneficial to extracting bridge frequencies from the vehicle response, by Lin and Yang (2005) experimentally and by Chang *et al*. (2010) numerically. The other approach is to suppress or eliminate the effect of road surface roughness, which will be presented after a general theory is formulated in the following section of the VBI problem considering the effect of road surface roughness.

6. Closed-form solution of vehicle response considering road surface roughness

It has been illustrated in preceding section that the vehicle passing a bridge will be excited more seriously by road surface roughness than by the bridge that is initially at rest. Such a phenomenon can be physically interpreted by the analytical formulation to be presented below.

Fig. 6 shows the two-dimensional vehicle-bridge interaction model of concern herein, where the vehicle is modeled as a moving sprung mass m_v supported by a spring of stiffness k_v, and the simple bridge is modeled as a Bernoulli-Euler beam of length L, mass density $\overline{m}$ per unit length, and bending rigidity EI. The road surface roughness profile is denoted by $r(x)$, a function of the bridge axis x. The damping effects of both the vehicle and bridge are neglected, since the responses considered herein are mainly of the transient nature, for which the damping effects can be ignored.

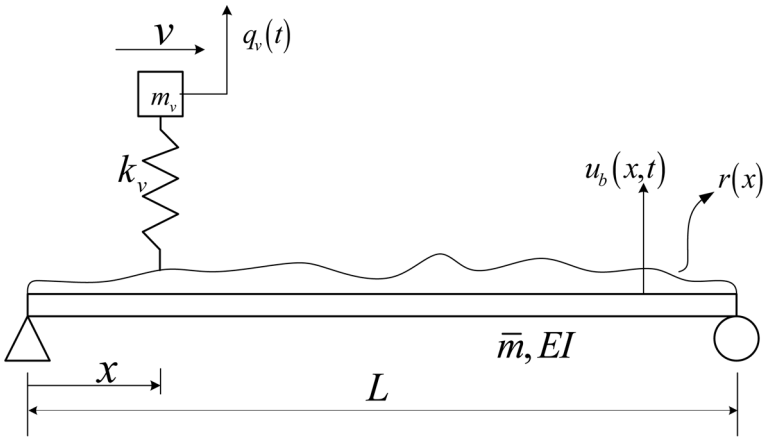

Fig. 6 Mathematical model

Let the vehicle move over the bridge with speed v. The equations of motion for both the vehicle and bridge at time t can be expressed as follows

$$m_v\ddot{q}_v(t) + k_v[q_v(t) - u_b(x, t)|_{x = vt} - r(x)|_{x = vt}] = 0 \tag{7}$$

$$\overline{m}\ddot{u}_b(x, t) + EIu_b''''(x, t) = f_c(t)\delta(x - vt) \tag{8}$$

where q_v and u_b denote the vertical displacement of the vehicle and bridge, respectively, and the contact force f_c is

$$f_c(t) = -m_v g + k_v[q_v(t) - u_b(x, t)|_{x = vt}] - k_v[r(x)|_{x = vt}] \tag{9}$$

It should be noted that the equations of motion in Eqs. (7) and (8) differ from those Yang *et al*. (2004) merely in the inclusion of the term related to road surface roughness, i.e., $-k_v\,[r\,(x)|_{x = vt}]$ in the contact force f_c.

By the modal superposition method, the bridge response can be expressed in terms of the modal shapes $\phi_n(x)$ and generalized coordinates $q_{b,n}(t)$. Furthermore, the modal shapes that satisfy the boundary conditions of the simple beam are of the sinusoidal form, $\sin(n\pi x / L)$. Consequently, the solution to the beam equation, Eq. (8), can be expressed as (Biggs 1964):

$$u(x, t) = \sum_{n = 1}^{\infty} \phi_n(x) q_{b,n}(t) = \sum_{n = 1}^{\infty} \sin\frac{n\pi x}{L} q_{b,n}(t) \tag{10}$$

Substituting Eq. (10) into Eq. (8) yields

$$\sum_{n = 1}^{\infty} \overline{m} \sin\frac{n\pi x}{L}\ddot{q}_{b,n}(t) + \sum_{n = 1}^{\infty} EI\left(\frac{n\pi}{L}\right)^4 \sin\frac{n\pi x}{L} q_{b,n}(t) = f_c\delta(x - vt) \tag{11}$$

Multiplying the above equation with modal shapes $\sin(n\pi x/L)$ and integrating the variable x from 0 to L, one obtains

$$\ddot{q}_{b,n} + \omega_{b,n}^2 q_b = 2\sin\left(\frac{n\pi vt}{L}\right)\left\{\frac{-m_v g}{\overline{m}L} + \frac{m_v\omega_v^2}{\overline{m}L}[q_v - u_b(x, t)|_{x = vt}] - \frac{m_v\omega_v^2}{\overline{m}L} r(x)|_{x = vt}\right\} \tag{12}$$

where $\omega_{b,n}$ is the bridge frequency of the nth mode and ω_v the vehicle frequency, which are respectively defined as

$$\omega_{b,n} = \frac{n^2\pi^2}{L^2}\sqrt{\frac{EI}{\overline{m}}} \tag{13}$$

$$\omega_v = \sqrt{\frac{k_v}{m_v}} \tag{14}$$

It should be noted the variations in the elastic force of the suspension and in the inertial force of the vehicle caused by the surface roughness, as represented by the penultimate and last term, respectively, on the right side of Eq. (12), have generally negligible effect on the response of the beam (Yau *et al*. 1999). By neglecting these two terms, the equation of motion for the beam in Eq. (12) reduces to

$$\ddot{q}_{b,n} + \omega_{b,n}^2 q_b = 2\sin\frac{n\pi vt}{L}\left\{\frac{-m_v g}{\overline{m}L}\right\} \tag{15}$$

Assuming zero initial conditions for the beam, one can solve Eq. (15) to obtain the generalized coordinate $q_{b,n}$ of the nth mode as

$$q_{b,n}(t) = \frac{\Delta_{st,n}}{1-S_n^2}\left[\sin\frac{n\pi vt}{L} - S_n \sin\omega_{b,n}t\right] \tag{16}$$

where $\Delta_{st,n}$ is the static deflection caused by the weight of the vehicle

$$\Delta_{st,n} = \frac{-2m_v g L^3}{n^4\pi^4 EI} \tag{17}$$

and S_n is a non-dimensional speed parameter

$$S_n = \frac{n\pi v}{L\omega_{b,n}} \tag{18}$$

Substituting Eq. (16) back into Eq. (10) yields the general solution of the vertical displacement of the bridge as

$$u(x,t) = \sum_n \frac{\Delta_{st,n}}{1-S_n^2}\left\{\sin\frac{n\pi x}{L}\left[\sin\frac{n\pi vt}{L} - S_n\sin\omega_{b,n}t\right]\right\} \tag{19}$$

It should be noted that, even with the neglect of the effect of road surface roughness, Eq. (19) is generally accurate for predicting the beam response (Yau *et al*. 1999).

At this stage, one can proceed to solve the vehicle response. First, the equation of motion for the vehicle in Eq. (7) may be re-written as

$$\ddot{q}_v(t) + \omega_v^2 q_v(t) = \omega_v^2 r(x)\big|_{x=vt} + \omega_v^2 u_b(x,t)\big|_{x=vt} \tag{20}$$

Clearly, the vehicle is subjected to two excitational sources: the bridge vibration and road surface roughness, as represented by the terms on the right hand side of Eq. (20). Substituting Eq. (19) for $u(x,t)$ and Eq. (3) for $r(x)$ into Eq. (20) and applying Duhamel's integral, the vehicle displacement can be obtained as

$$q_v(t) = \sum_{n=1}^{\infty}\left\{A_{1,n}\cos\left(\frac{(n-1)\pi v}{L}\right)t + A_{2,n}\cos\left(\frac{(n+1)\pi v}{L}\right)t + A_{3,n}\cos(\omega_v t)\right.$$

$$\left. + A_{4,n}\cos\left(\omega_{b,n} - \frac{n\pi v}{L}\right)t + A_{5,n}\cos\left(\omega_{b,n} + \frac{n\pi v}{L}\right)t\right\}$$

$$+ \sum_{i=1}\frac{\omega_v^2 d_i}{\omega_v^2 - (n_{s,i}v)^2}\left[\cos(n_{s,i}vt + \theta_i) - \cos(\theta_i)\cos(\omega_v t) + \frac{n_{s,i}v}{\omega_v}\sin(\theta_i)\sin(\omega_v t)\right] \tag{21}$$

where the coefficients are

$$A_{1,n} = \frac{\Delta_{st,n}\omega_v^2}{2(1-S_n^2)\left(\omega_v + \frac{(n-1)\pi v}{L}\right)\left(\omega_v - \frac{(n-1)\pi v}{L}\right)} \tag{22a}$$

$$A_{2,n} = \frac{-\Delta_{st,n}\omega_v^2}{2(1-S_n^2)\left(\omega_v + \frac{(n+1)\pi v}{L}\right)\left(\omega_v - \frac{(n+1)\pi v}{L}\right)} \tag{22b}$$

$$\begin{aligned} A_{3,n} = & \frac{2\Delta_{st,n}\omega_v^2\left(\frac{\pi v}{L}\right)^2 n}{2(1-S_n^2)\left(\omega_v + \frac{(n-1)\pi v}{L}\right)\left(\omega_v - \frac{(n-1)\pi v}{L}\right)\left(\omega_v + \frac{(n+1)\pi v}{L}\right)\left(\omega_v - \frac{(n+1)\pi v}{L}\right)} \\ & - \frac{2\Delta_{st,n}S_n\omega_v^2\left(\frac{nvv}{L}\right)\omega_{b,n}}{\left(\omega_v - \omega_{b,n} + \frac{n\pi v}{L}\right)\left(\omega_v + \omega_{b,n} - \frac{n\pi v}{L}\right)\left(\omega_v + \omega_{b,n} + \frac{n\pi v}{L}\right)\left(\omega_v - \omega_{b,n} - \frac{n\pi v}{L}\right)} \end{aligned} \tag{22c}$$

$$A_{4,n} = \frac{-S_n\Delta_{st,n}\omega_v^2}{2(1-S_n^2)\left(\omega_v - \omega_{b,n} + \frac{n\pi v}{L}\right)\left(\omega_v + \omega_{b,n} - \frac{n\pi v}{L}\right)} \tag{22d}$$

$$A_{5,n} = \frac{S_n\Delta_{st,n}\omega_v^2}{2(1-S_n^2)\left(\omega_v + \omega_{b,n} + \frac{n\pi v}{L}\right)\left(\omega_v - \omega_{b,n} - \frac{n\pi v}{L}\right)} \tag{22e}$$

Differentiating Eq. (21) with respect to t twice, the vehicle acceleration response can be obtained as

$$\begin{aligned} \ddot{q}_v(t) = & \sum_{n=1}^{\infty}\left\{\bar{\bar{A}}_{1,n}\cos\left(\frac{(n-1)\pi v}{L}\right)t + \bar{\bar{A}}_{2,n}\cos\left(\frac{(n+1)\pi v}{L}\right)t + \bar{\bar{A}}_{3,n}\cos(\omega_v t)\right. \\ & \left. + \bar{\bar{A}}_{4,n}\cos\left(\omega_{b,n} - \frac{n\pi v}{L}\right)t + \bar{\bar{A}}_{5,n}\cos\left(\omega_{b,n} + \frac{n\pi v}{L}\right)t\right\} \\ & + \sum_{i=1}\frac{\omega_v^2 d_i}{\omega_v^2 - (n_{s,i}v)^2}[-(n_{s,i}v)^2\cos(n_{s,i}vt + \theta_i) + \omega_v^2\cos(\theta_i)\cos(\omega_v t) - (n_{s,i}v\omega_v)\sin(\theta_i)\sin(\omega_v t)] \end{aligned} \tag{23}$$

where the coefficients are

$$\bar{\bar{A}}_{1,n} = -\left(\frac{(n-1)\pi v}{L}\right)^2 \times A_{1,n}, \quad \bar{\bar{A}}_{2,n} = -\left(\frac{(n+1)\pi v}{L}\right)^2 \times A_{2,n}, \quad \bar{\bar{A}}_{3,n} = -\omega_v^2 \times A_{3,n},$$

$$\bar{\bar{A}}_{4,n} = -\left(\omega_{b,n} - \frac{n\pi v}{L}\right)^2 \times A_{4,n}, \quad \bar{\bar{A}}_{5,n} = -\left(\omega_{b,n} + \frac{n\pi v}{L}\right)^2 \times A_{5,n} \tag{24a-e}$$

As can be seen from Eq. (23), besides the following three groups of frequency that have been identified in the vehicle response by Yang and Lin (2005): driving frequencies $(n \pm 1)\pi v / L$, bridge-related frequencies $\omega_{b,n} \pm n\pi v / L$, and vehicle frequency ω_v, the vehicle acceleration response is also affected by the roughness-related frequencies $n_{s,i}v$, defined as the product of the spatial frequency $n_{s,i}$ of road surface roughness and the vehicle speed v. The solution for the vehicle acceleration response in Eq. (23) differs from the one by Yang and Lin (2005) in the appearance of the terms due to road surface roughness, which are denoted as $\ddot{q}_{v,r}$, namely,

$$\ddot{q}_{v,r} = \sum_{i=1} \frac{\omega_v^2 d_i}{\omega_v^2 - (n_{s,i}v)^2}[-(n_{s,i}v)^2 \cos(n_{s,i}vt + \theta_i) + \omega_v^2 \cos(\theta_i)\cos(\omega_v t) - (n_{s,i}v\omega_v)\sin(\theta_i)\sin(\omega_v t)] \tag{25}$$

The preceding equation indicates that the roughness term $\ddot{q}_{v,r}$ is dominated by the roughness frequencies $n_{s,i}v$ and vehicle frequency ω_v. This term has the function of introducing the roughness frequencies to the vehicle response, while amplifying the amplitudes of the vehicle frequency, especially when any of the roughness frequencies $n_{s,i}v$ is close to the vehicle frequency ω_v, as revealed by the denominator in Eq. (25). Both effects are unfavorable to identification of bridge frequencies from the vehicle response. Evidently, the present closed-form solution offers a theoretical basis for interpreting the influence of road surface roughness on the vehicle response, as observed from the numerical analyses presented in previous sections.

7. Reducing the impact of road surface roughness by using two vehicles

From Eq. (20), it is clear that the test vehicle is subjected to two excitational sources: the bridge vibration (as represented by the term $m_v \times \omega_v^2 u_b(x, t)|_{x=vt}$) and road surface roughness (as represented by the term $m_v \times \omega_v^2 r(x)|_{x=vt}$). As was stated previously, to enhance the visibility of bridge frequencies from the vehicle spectrum, one approach is to amplify the bridge vibration by letting the bridge be exposed to existing traffic or accompanying vehicles (Yang and Lin 2005, Chang *et al*. 2010), which is not the focus of the present study.

The other approach is to reduce the impact of road surface roughness by recording the responses of two connected vehicles during their passage over the same bridge, and then by deducting the response recorded for one vehicle from that of the other vehicle to eliminate the effect of road surface roughness (Yang *et al*. 2012). The latter approach has been verified to be feasible in the numerical simulation using the VBI element. In this section, a theoretical formulation along with physical interpretation will be presented for such an approach. The mathematical model considered for the problem is shown in Fig. 7, in which two connected test vehicles with fixed spacing s pass through a simple bridge at constant speed v. The rear vehicle is labeled as 1 and the front one as 2. The symbols used for the bridge and vehicle are identical to those previously introduced.

The equations of motion for both vehicles can be expressed as follows.

$$m_{v,1}\ddot{q}_{v,1}(t) + k_{v,1}[q_{v,1}(t) - u_b(x, t)|_{x=vt} - r(x)|_{x=vt}] = 0 \tag{26}$$

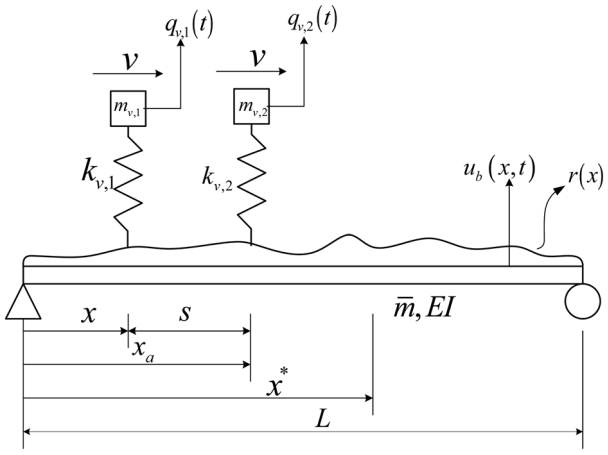

Fig. 7 Model of two connected vehicles passing through a simple bridge

$$m_{v,2}\ddot{q}_{v,2}(t) + k_{v,2}[q_{v,2}(t) - u_b(x,t)|_{x=vt_a} - r(x)|_{x=vt_a}] = 0 \tag{27}$$

where the time variable t_a for the front vehicle is defined as the sum of time t and the delay t_s

$$t_a \equiv t + \frac{s}{v} = t + t_s \tag{28}$$

The equation of motion for the bridge is

$$\overline{m}\ddot{u}_b(x,t) + EIu_b''''(x,t) = f_{c,1}(t)\delta(x - vt) + f_{c,2}(t)\delta(x - vt_a) \tag{29}$$

where $f_{c,1}$ and $f_{c,2}$ are the contact forces for the rear and front vehicles, respectively,

$$f_{c,1} = -m_{v,1}g + k_{v,1}[q_{v,1}(t) - u_b(x,t)|_{x=vt} - r(x)|_{x=vt}] \tag{30}$$

$$f_{c,2} = -m_{v,2}g + k_{v,2}[q_{v,2}(t) - u_b(x,t)|_{x=vt_a} - r(x)|_{x=vt_a}] \tag{31}$$

By the modal superposition method, one can substitute the bridge displacement in Eq. (10) into Eq. (29) to obtain

$$\sum_{n=1}^{\infty} \overline{m}\sin\frac{n\pi x}{L}\ddot{q}_{b,n}(t) + \sum_{n=1}^{\infty} EI\left(\frac{n\pi}{L}\right)^4 \sin\frac{n\pi x}{L}q_{b,n}(t) = f_{c,1}\delta(x - vt) + f_{c,2}\delta(x - vt_a) \tag{32}$$

Multiplying the preceding equation with $\sin(n\pi x/L)$ and integrating x from 0 to L yields the following equation

$$\ddot{q}_{b,n} + \omega_{b,n}^2 q_b = 2\sin\frac{n\pi vt}{L}\left\{\frac{-m_{v,1}g}{\overline{m}L} + \frac{m_{v,1}\omega_{v,1}^2}{\overline{m}L}[q_{v,1}(t) - u_b(x,t)|_{x=vt} - r(x)|_{x=vt}]\right\}$$
$$+ 2\sin\frac{n\pi vt_a}{L}\left\{\frac{-m_{v,2}g}{\overline{m}L} + \frac{m_{v,2}\omega_{v,2}^2}{\overline{m}L}[q_{v,2}(t) - u_b(x,t)|_{x=vt_a} - r(x)|_{x=vt_a}]\right\} \tag{33}$$

where $\omega_{b,n}$ is the bridge frequency of nth mode, as defined in Eq. (13), and $\omega_{v,j}$ is the frequency of the rear ($j = 1$) or front vehicle ($j = 2$), defined as

$$\omega_{v,j} = \sqrt{\frac{k_{v,j}}{m_{v,j}}} \tag{34}$$

Similarly, as far as the bridge response is concerned, the terms inside the brackets of Eq. (33) are negligibly small compared with their preceding terms. Thus, Eq. (33) can be reduced as

$$\ddot{q}_{b,n} + \omega_{b,n}^2 q_{b,n} = 2\sin\frac{n\pi vt}{L}\left\{\frac{-m_{v,1}g}{\bar{m}L}\right\} + 2\sin\frac{n\pi vt_a}{L}\left\{\frac{-m_{v,2}g}{\bar{m}L}\right\} \tag{35}$$

Solving the above equation yields the generalized coordinate of the nth mode as

$$\begin{aligned} q_{b,n}(t) = {} & \frac{-\Delta_{st,n}^2}{1-S_n^2}\sin\frac{n\pi vt_s}{L}\cos\omega_{b,n}t - S_n\left[\frac{\Delta_{st,n}^1}{1-S_n^2} + \frac{\Delta_{st,n}^2}{1-S_n^2}\cos\frac{n\pi vt_s}{L}\right]\sin\omega_{b,n}t \\ & + \left[\frac{\Delta_{st,n}^1}{1-S_n^2} + \frac{\Delta_{st,n}^2}{1-S_n^2}\cos\frac{n\pi vt_s}{L}\right]\sin\frac{n\pi vt}{L} + \left[\frac{\Delta_{st,n}^2}{1-S_n^2}\sin\frac{n\pi vt_s}{L}\right]\cos\frac{n\pi vt}{L} \end{aligned} \tag{36}$$

where S_n is the speed parameter as defined in Eq. (18), and $\Delta_{st,n}^j$ is the static displacement induced by the rear ($j = 1$) or front vehicle ($j = 2$)

$$\Delta_{st,n}^j = \frac{-2m_{v,j}gL^3}{n^4\pi^4 EI} \tag{37}$$

Substituting Eq. (36) back to Eq. (10) yields the general bridge displacement

$$\begin{aligned} u_b(x,t) = {} & \sum_{n=1}^{\infty}\left\{\frac{\Delta_{st,n}^1}{1-S_n^2}\sin\frac{n\pi x}{L}\left[\sin\frac{n\pi vt}{L} - S_n\sin\omega_{b,n}t\right]\right\} \\ & + \sum_{n=1}^{\infty}\left\{\frac{\Delta_{st,n}^2}{1-S_n^2}\sin\frac{n\pi x}{L}\left[\sin\frac{n\pi vt_a}{L} - \sin\frac{n\pi vt_s}{L}\cos\omega_{b,n}t - S_n\cos\frac{n\pi vt_s}{L}\sin\omega_{b,n}t\right]\right\} \end{aligned} \tag{38}$$

The preceding equation is an approximate, but quite accurate, expression of the bridge displacement when subjected to two connected vehicles passing over the bridge with constant speed and spacing. Clearly, the first braced term is contributed by the rear vehicle and the second braced term by the front vehicle.

With the bridge response made available, the responses of the two vehicles can be solved as follows. First, the equation of motion for the rear vehicle can be re-written as

$$\ddot{q}_{v,1} + \omega_{v,1}^2 q_{v,1} = \omega_{v,1}^2 r(x)\big|_{x=vt} + \omega_{v,1}^2 u_b(x,t)\big|_{x=vt} \tag{39}$$

Substituting Eq. (3) for $r(x)$ and Eq. (38) for $u_b(x,t)$ into the preceding equation, the displacement

of the rear vehicle can be solved. Herein, only the part of the response induced by road surface roughness is of our concern, which can be given as follows

$$q_{v1,r}(t) = \sum_{i=1}^{\infty} d_i \frac{\omega_{v,1}^2}{\omega_{v,1}^2 - (n_{s,i}v)^2}\left[\cos(n_{s,i}vt + \theta_i) - \cos\theta_i \cos\omega_{v,1}t + \frac{n_{s,i}v}{\omega_{v,1}}\sin\theta_i \sin\omega_{v,1}t\right] \quad (40)$$

Differentiating twice with respect to t yields the acceleration of the rear vehicle as

$$\ddot{q}_{v1,r}(t) = \sum_{i=1}^{\infty} d_i \frac{\omega_{v,1}^2}{\omega_{v,1}^2 - (n_i v)^2}[-(n_i v)^2 \cos(n_i vt + \theta_i) + \omega_{v,1}^2 \cos\theta_i \cos\omega_{v,1}t - (n_i v\omega_{v,1})\sin\theta_i \sin\omega_{v,1}t] \quad (41)$$

Similar to Eq. (25), $\ddot{q}_{v1,r}$ is governed by the roughness frequencies $n_{s,i}v$ and vehicle frequency ω_v. Let us denote the component related to the roughness frequencies as $\ddot{R}_{1,r}$

$$\ddot{R}_{1,r}(t) = \sum_{i=1}^{\infty} d_i \frac{\omega_{v,1}^2}{\omega_{v,1}^2 - (n_i v)^2}[-(n_i v)^2 \cos(n_i vt + \theta_i)] \quad (42)$$

It is known that $\ddot{R}_{1,r}$ may overshadow the bridge frequency related components in the vehicle spectrum, and making them difficult to be identified.
Similarly, the acceleration of the front vehicle due to road surface roughness is

$$\ddot{q}_{v2,r}(t) = \sum_{i=1}^{\infty} d_i \frac{\omega_{v,2}^2}{\omega_{v,2}^2 - (n_i v)^2}[-(n_i v)^2 \cos(n_i vt + \theta_a) + \omega_{v,2}^2 \cos\theta_a \cos\omega_{v,2}t - (n_i v\omega_{v,2})\sin\theta_a \sin\omega_{v,2}t] \quad (43)$$

and the part of response $\ddot{R}_{2,r}$ directly related to roughness frequencies is

$$\ddot{R}_{2,r}(t) = \sum_{i=1} d_i \frac{\omega_{v,2}^2}{\omega_{v,2}^2 - (n_i v)^2}[-(n_i v)^2 \cos(n_i vt + \theta_a)] \quad (44)$$

where the phase angle θ_a is defined as $\theta_a = n_i(vt_s) + \theta_i = n_i s + \theta_i$.

A comparison of the roughness responses for $\ddot{R}_{1,r}$ and $\ddot{R}_{2,r}$ in Eqs. (42) and (44) indicates that their amplitudes $A_{1r,i}$ and $A_{2r,i}$ have similar expressions

$$A_{1r,i} = \left| d_i \frac{\omega_{v,1}^2 (n_i v)^2}{\omega_{v,1}^2 - (n_i v)^2} \right| \quad (45)$$

$$A_{2r,i} = \left| d_i \frac{\omega_{v,2}^2 (n_i v)^2}{\omega_{v,2}^2 - (n_i v)^2} \right| \quad (46)$$

Specifically, they are equal to each other when $\omega_{v,1} = \omega_{v,2} = \omega_v$

$$A_{1r,i} = A_{2r,i} = \left| d_i \frac{\omega_v^2 (n_i v)^2}{\omega_v^2 - (n_i v)^2} \right| \tag{47}$$

Theoretically, the above equality offers an attractive clue for reducing the effect of road surface roughness. Namely, for two vehicles of identical frequency, i.e., $\omega_{v,1} = \omega_{v,2} = \omega_v$, passing through the bridge with the same roughness profile, their response amplitudes associated with roughness frequencies are same and therefore can be eliminated by subtracting one response spectrum from the other, which offers the theoretical basis for the idea proposed by Yang *et al*. (2012).

Moreover, for two vehicles with identical frequency, the responses $\ddot{R}_{1,r}$ and $\ddot{R}_{2,r}$ in Eqs. (42) and (44) differ only in the phase angle term, i.e., with θ_i for $\ddot{R}_{1,r}$ and θ_a for $\ddot{R}_{2,r}$, meaning that the roughness frequency-related components for the two vehicles are identical when evaluated at the same position x^*, but with a time delay s/v. This can be proved by letting $t_1^* = x^*/v$ and $t_2^* = t_1^* - s/v$ for the rear and front vehicle, respectively, and showing that the results obtained from Eqs. (42) and (44) for $\ddot{R}_{1,r}$ and $\ddot{R}_{2,r}$ are identical. As a result, one may also work on the time domain to eliminate the effect of surface roughness, by first synchronizing the accelerations of the two vehicles for the same contact points, and then subtracting the synchronized responses from each other.

8. Numerical studies

It has been theoretically proved in preceding section that the effect of road surface roughness can be eliminated by adopting two vehicles of identical frequency and by subtracting the response of one vehicle from the other. The feasibility of such an idea will be illustrated through several examples in this section. The properties adopted of the simple bridge remain the same as those previously used: $L = 30$ m, $E = 27.5$ GPa, $I_b = 0.175$ m^4, $\overline{m} = 1000$ kg/m and $A = 2$ m^2.

8.1 Example 1. Two identical vehicles passing through the bridge of road surface Class A

To ensure the frequencies to be the same, two vehicles with the following identical properties are adopted: $m_{v,1} = m_{v,2} = 1000$ kg, $k_{v,1} = k_{v,2} = 170$ kN/m. They move with speed $v = 2$ m/s and spacing $s = 3$ m over the bridge of road surface class A, i.e., the best quality. Fig. 8(a) shows the amplitude spectrum of the acceleration response calculated of the rear vehicle, in which only the vehicle frequency f_v, but no bridge-related frequencies, can be identified. As was stated previously, the difficulty in bridge frequency identification from the vehicle spectrum is mainly due to the fact that the roughness-induced responses are so large that the bridge-induced responses are overshadowed.

To reduce the effect of surface roughness in time domain, one first synchronizes the acceleration responses of the two vehicles with respect to identical contact points, and then subtracts the synchronized response for one vehicle from the other. Fig. 8(b) shows the amplitude spectrum of the subtracted response. As can be seen, the effect of roughness has been largely reduced, making it easier to identify the bridge frequencies of the first and second modes, $f_{b,1}$ and $f_{b,2}$, for this example.

8.2 Example 2. Two identical vehicles passing through the bridge of road surface Class C

In this example, all the properties adopted for the bridge and vehicle are identical to those of

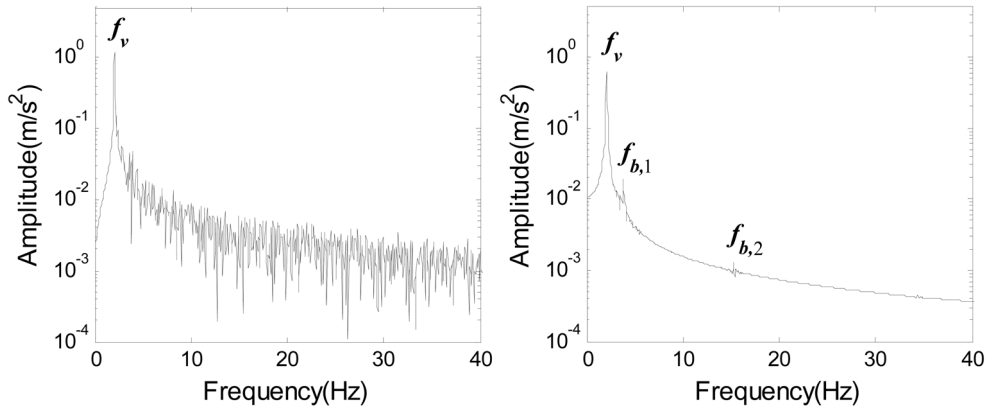

Fig. 8 Example 1: Acceleration response spectrum of rear vehicle: (a) original and (b) subtracted

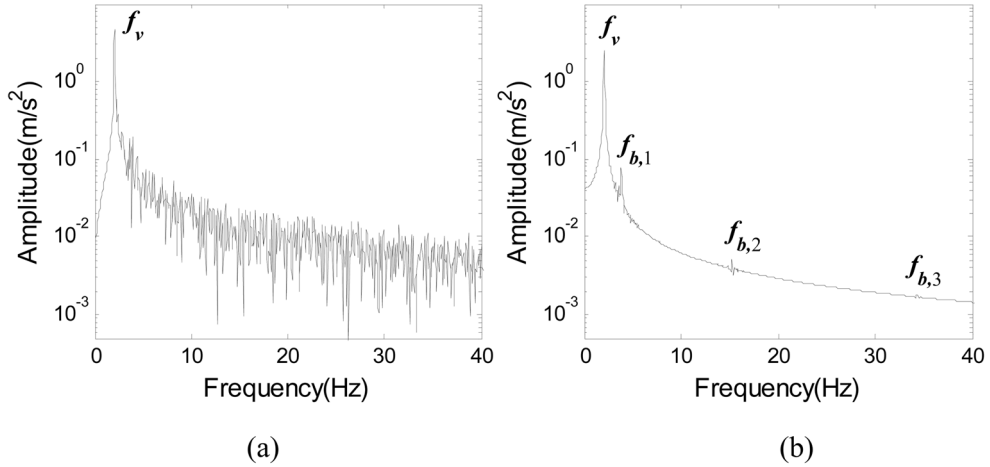

Fig. 9 Example 2: Acceleration response spectrum of rear vehicle: (a) original and (b) subtracted

Example 1, except that road surface class C (normal quality) is adopted. Figs. 9(a) and (b) respectively show the original and subtracted amplitude spectra of the acceleration response of the rear vehicle. Once again, these figures indicate that the effect of road surface roughness can be largely reduced by subtracting the response obtained for one vehicle from the other. For this example, the first three bridge frequencies, $f_{b,1}$ to $f_{b,3}$, can be clearly identified, even with a poorer road surface condition.

8.3 Example 3. Two vehicles of identical frequency but different properties

It was shown in Eqs. (42) and (44) that the vehicle responses induced by road surface roughness of the same profile are identical, if the two vehicles adopted are of identical frequency. Certainly,

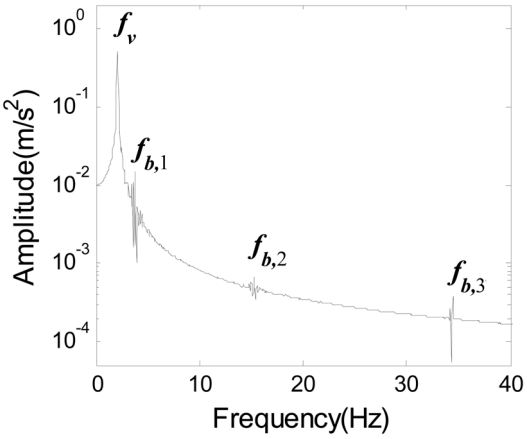

Fig. 10 Example 3: Subtracted amplitude spectrum of the response

for two vehicles to have the same frequency, one may just adopt two vehicles of the same physical properties, which are exactly the cases in Examples 1 and 2. In this example, two vehicles of identical frequency, but of different physical properties, will be adopted. To this end, the same physical properties are adopted for the rear vehicle: $m_{v,1}$ = 1000 kg and $k_{v,1}$ = 170 kN/m, but the front vehicle is assumed to be much lighter and softer, $m_{v,2}$ = 100 kg and $k_{v,2}$ = 17 kN/m. It is easy to see that both vehicles have an identical frequency of 2.08 Hz. We shall let the two vehicles move over the bridge with constant speed v = 2 m/s and spacing s = 3 m.

Fig. 10 shows the amplitude spectrum of the response obtained by subtracting the synchronized acceleration response of the front vehicle from that of the rear vehicle. This figure indicates that as long as two vehicles have identical frequency, the effect of road surface roughness can be largely reduced through subtraction, so as to enhance the visibility of the bridge frequencies, even though the two vehicles are physically different.

8.4 Example 4. Effect of vehicle spacing on identification of bridge frequencies

In this example, the effect of vehicle spacing on the accuracy of the bridge frequencies identified will be studied. Two identical vehicles are adopted, with the same properties as those adopted in Example 1. They are allowed to pass at constant speed v = 2 m/s through the simple bridge with road surface of Class A. The spacing s between the two vehicles varies from 3 to 15 m, as listed in Table 1.

Fig. 11 shows the amplitude spectrum of the subtracted response for the five cases considered, and Table 2 summarizes the bridge and vehicle frequencies identified. It is observed in each case that the effect of road surface roughness can be reduced, thereby making it easier to identify the bridge frequencies. No obvious discrepancy in the amplitude spectra and bridge frequencies identified is observed as far as the visibility of bridge frequencies is concerned. This result indicates that vehicle spacing is not a key parameter concerning the visibility of bridge frequencies. However, the spacing between two connected vehicles is a mechanical issue that should be studied from the point of maneuverability or dynamic stability, to ensure that the two connected vehicles can move smoothly together at certain speeds in practice.

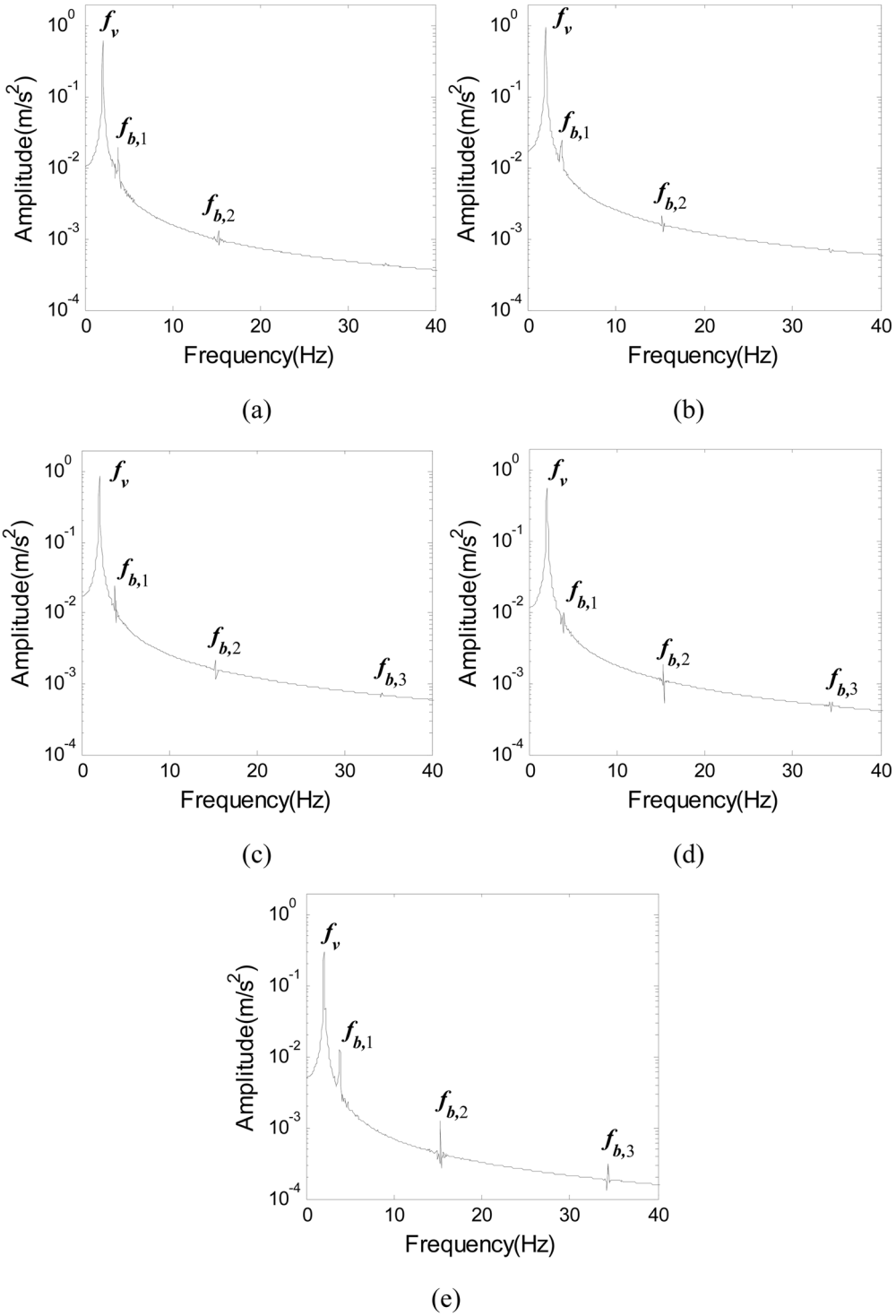

Fig. 11 Amplitude spectrum of the subtracted response: (a) Case 1, (b) Case 2, (c) Case 3, (d) Case 4 and (e) Case 5

Table 1 Vehicle spacings adopted in Example 4

Case	s (m)	s/L (%)
1	3	10
2	6	20
3	9	30
4	12	40
5	15	50

Table 2 Bridge and vehicle frequencies identified

Case	s (m)	$f_{b,1}$ (Hz)*	$f_{b,2}$ (Hz)*	$f_{b,3}$ (Hz)*	f_v (Hz)**
1	3	3.83	15.37	34.53	2.07
2	6	3.80	15.37	34.37	2.07
3	9	3.77	15.37	34.33	2.07
4	12	3.90	15.30	34.33	2.07
5	15	3.90	15.30	34.33	2.07

Note: *Analytical bridge frequencies of the first three modes: 3.83, 15.32 and 34.46 Hz.
**Analytical vehicle frequency: 2.08 Hz.

9. Conclusions

The effect of road surface roughness on the response of a moving vehicle aimed at the visibility of bridge frequencies is studied herein by an analytical approach. Firstly, from the numerical simulations using the vehicle-bridge interaction element, it is illustrated that road surface roughness is an effect of crucial importance, which may excite the vehicle to a level higher than the bridge in vibration, such that the former frequency components may overshadow the latter in the vehicle spectrum.

The effect of road surface roughness is also investigated by an approximate, but quite accurate, theory in closed form, from which the influences of two excitational sources to the vehicle, i.e., surface roughness and bridge in vibration, can be clearly interpreted. The theory is then expanded to include the effect of an accompanying moving vehicle. From the analysis, it is concluded that, if two vehicles of identical frequency pass at constant speed through the same profile of road surface roughness, the roughness frequency-related responses for the two vehicles should be identical when traveling to the same position, but differ by a phase angle. Consequently, one can work on the time domain to eliminate the effect of road surface roughness by first synchronizing the responses of the two vehicles with respect to the same contact points, and then by subtracting the synchronized response of one vehicle from the other. The two vehicles should be of identical frequency, but can possess different physical properties. The feasibility of the proposed method is verified in several numerical examples, even with road surface of normal class. Finally, it was numerically demonstrated that vehicle spacing is not a key parameter for identification of bridge frequencies; it should be determined according to the maneuverability or dynamic stability of the two vehicles in connection, such that they can move smoothly together at certain speeds in practice.

Acknowledgments

The research reported herein is sponsored in part by the National Science Council (ROC) through grant number NSC 100-2221-E-224-045-MY2. The assistance from Tongji University (973 program, Ministry of Science and Technology, PRC) should also be acknowledged.

References

Abdel-Ghaffar, A.M. and Scanlan, R.H. (1985), "Ambient vibration studies of Golden Gate Bridge: I. suspended structure", *J. Eng. Mech.-ASCE*, **111**(4), 462-482.

Biggs, J.M. (1964), *Introduction to structural dynamics*, McGraw-Hill, New York.

Brownjohn, J.M.W., Magalhaes, F., Caetano, E. and Cunha, A. (2010), "Ambient vibration re-testing and operational modal analysis of the Humber Bridge", *Eng. Struct.*, **32**(8), 2003-2018.

Bu, J.Q., Law, S.S. and Zhu, X.Q. (2006), "Innovative bridge condition assessment from dynamic response of a passing vehicle", *J. Eng. Mech.-ASCE*, **132**(12), 1372-1379.

Chang, K.C., Wu, F.B. and Yang, Y.B. (2010), "Effect of road surface roughness on indirect approach for measuring bridge frequencies from a passing vehicle", *Interact. Multiscale Mech.*, **3**(4), 299-308.

He, X., Moaveni, B., Conte, J.P., Elgamal, A. and Masri, S.F. (2009), "System identification of Alfred Zampa Memorial Bridge using dynamic field test data", *J. Struct. Eng.-ASCE*, **135**(1), 54-66.

ISO 8608 (1995), *Mechanical vibration-road surface profiles - Reporting of measured data*, Geneva, Switzerland.

Lin, C.W. and Yang, Y.B. (2005), "Use of a passing vehicle to scan the bridge frequencies - an experimental verification", *Eng. Struct.*, **27**(13), 1865-1878.

McGetrick, P.J., Gonzalez, A. and OBrien, E.J. (2009), "Theoretical investigation of the use of a moving vehicle to identify bridge dynamic parameters", *Insight*, **51**(8), 433-438.

Nguyen, K.V. and Tran, H.T. (2010), "Multi-cracks detection of a beam-like structure based on the on-vehicle vibration signal and wavelet analysis", *J. Sound Vib.*, **329**(21), 4455-4465.

Ren, W.X., Zhao, T. and Harik, I.E. (2004), "Experimental and analytical modal analysis of steel arch bridge", *J. Struct. Eng.-ASCE*, **130**(7), 1022-1031.

Wilson, J.C. and Liu, T. (1991), "Ambient vibration measurements on a cable-stayed bridge", *Earthq. Eng. Struct. D.*, **20**(8), 723-747.

Xiang, Z., Dai, X., Zhang, Y. and Lu, Q. (2010), "The tap-scan method for damage detection of bridge structures", *Interact. Multiscale Mech.*, **3**(2), 173-191.

Yang, Y.B. and Chang, K.C. (2009a), "Extracting the bridge frequencies indirectly from a passing vehicle: parametric study", *Eng. Struct.*, **31**(10), 2448-2459.

Yang, Y.B. and Chang, K.C. (2009b), "Extraction of bridge frequencies from the dynamic response of a passing vehicle enhanced by the EMD technique", *J. Sound Vib.*, **322**(4-5), 718-739.

Yang, Y.B. and Lin, C.W. (2005), "Vehicle-bridge interaction dynamics and potential applications", *J. Sound Vib.*, **284**(1-2), 205-226.

Yang, Y.B., Li, Y.C. and Chang, K.C. (2012), "Using two connected vehicles to measure the frequencies of bridges with rough surface: a theoretical study", *Acta Mech.*, **223**(8), 1851-1861.

Yang, Y.B., Lin, C.W. and Yau J.D. (2004), "Extracting bridge frequencies from the dynamic response of a passing vehicle", *J. Sound Vib.*, **272**(3-5), 471-493.

Yau, J.D., Yang, Y.B. and Kuo, S.R. (1999), "Impact response of high speed rail bridges and riding comfort of rail cars", *Eng. Struct.*, **21**(9), 836-844.